Available online at www.sciencedirect.com
ScienceDirect
Coordination Chemistry Reviews 252 (2008) 2209–2223
COORDINATION CHEMISTRY REVIEWS
www.elsevier.com/locate/ccr

Review

Vanadium NMR of organovanadium complexes

Dieter Rehder *

Chemistry Department, University of Hamburg, Martin-Luther-King-Platz 6, 20146 Hamburg, Germany

Received 11 October 2007; accepted 7 January 2008
Available online 16 January 2008

Contents

Abstract

A brief (and simplified) introduction into the background theory of NMR parameters (shielding, scalar coupling constants, and relaxation times) pertinent to the quadrupolar nucleus ^{51}V is provided. General trends are discussed in the light of electronic and steric factors, medium effects, temperature and isotope effects influencing these parameters, in particular ^{51}V shielding. Data are reported on vanadium complexes containing at least one vanadium-to-carbon bond, including alkyl, alkylidene and alkylidyne complexes, complexes containing η^2- and η^3-bonded ligands, carbonyl and isonitrile complexes, as well as η^5-cyclopentadienyl and related vanadium compounds. DFT supported correlations between substituent effects and shielding, applicable to catalyst design, are included. The review focuses on solution NMR, but NMR in the crystalline solid state and in mesophases is also briefly addressed.

Keywords: Vanadium NMR; Organovanadium compounds; Carbonyl complexes; Catalysis

1. Introduction

Vanadium has been one of the earliest transition metal nuclei to be investigated systematically by NMR. This is not so much a consequence of the availability of a sufficiently large amount of suitable vanadium complexes, but essentially reflects the very appropriate NMR properties of this nucleus (Table 1), allowing for its detection at low concentrations and on simple instruments equipped with, e.g., a ^{13}C probe. This does not imply that ^{51}V NMR spectroscopy has remained on a simplistic level: new methods, also addressed in this review as far as the vanadium–carbon bond is involved, include two-dimensional spectroscopies, NMR in the solid state (static and MAS) and in mesophases, and the use of density functional calculations to predict catalytic activity and to reveal active intermediates in vanadium-catalysed organic reactions.

* Tel.: +49 40 42838 6087; fax: +49 40 42838 2882.
E-mail address: rehder@chemie.uni-hamburg.de.

0010-8545/$ – see front matter © 2008 Elsevier B.V. All rights reserved.
doi:10.1016/j.ccr.2008.01.008

Table 1
NMR parameters of naturally occurring vanadium nuclei[a]

Nucleus	N (%)	γ ($\times 10^7$ rad s^{-1} T^{-1})	Nuclear spin	Q (fm^2)	r (relative ^{13}C)	ν (at 2.35T[b]) (MHz)
^{50}V	0.25	+2.6721	6	+21	0.76	9.988
^{51}V	99.75	+7.0492	7/2	−4.8	2170	26.350

[a] N, natural abundance; γ, magnetogyric ration; Q, nuclear electric quadrupole moment; r, receptivity; ν, measuring frequency.
[b] ^{1}H of TMS resonates at 100 MHz.

Table 2
Solvent isotope effects Δ^D (per ^{2}H) for hexacarbonylvanadate $[V(CO)_6]^-$ [4]

Solvent	D_2O	CH_3OD	CD_3OH	THF[D8]	CD_3CN	Toluene[D8]
Counter-ion	$[Na(D_2O)_n]^+$	$[Et_4N]^+$	$[Et_4N]^+$	$[Et_4N]^+$	$[Et_4N]^+$	$[Me(decyl)_3N]^+$
Δ^D	−0.60	−0.21	−0.10	−0.09	−0.03	−0.01

The minus sign refers to additional shielding (upfield shift with respect to the B_0 field). Relative to the same sample in non-deuterated solvent.

The nucleus ^{51}V has a high natural abundance of 99.75%, and high receptivity, outdating that of ^{13}C by a factor of more than 2000. With a spin = 7/2, it belongs to the quadrupolar nuclei, with a comparatively (and conveniently) low nuclear quadrupole moment, giving rise to reasonably narrow resonance lines even in complexes of other than cubic symmetry, and thus to high resolution, allowing, in several cases, for resolved nuclear spin–spin coupling patterns. The shift range (Fig. 1), reflecting the sensitivity of the ^{51}V nucleus to electronic influences imparted by the coordination environment, spans almost 5000 ppm, i.e. even minor variations in the electronic situation are detectable through distinct variations of the chemical shifts. The second naturally occurring vanadium isotope, the nucleus ^{50}V, is mildly radioactive (half life 17.1 billion years; the decay is mainly by electron capture/positron emission). Its nuclear properties are certainly less favourable, and this nucleus has not found broad application and none in organovanadium chemistry. Vanadium NMR has been reviewed several times; for more recent reviews see Refs. [1,2], for reviews directed towards organovanadium compounds see Ref. [3].

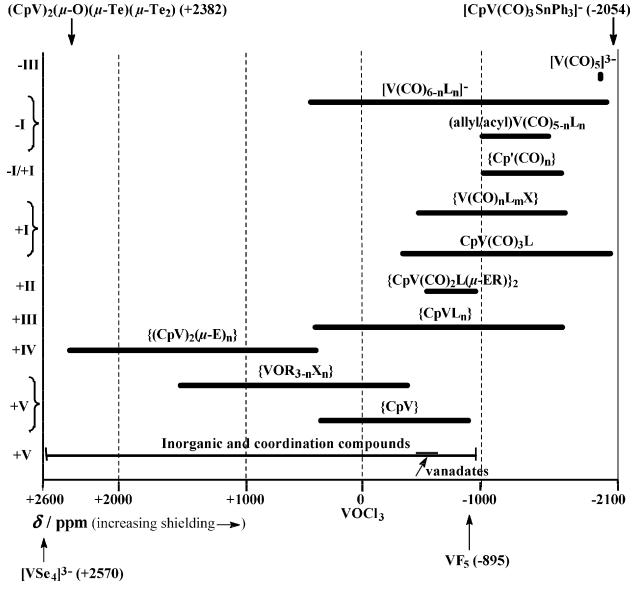

Fig. 1. Shift ranges covered by selected families of vanadium compounds. Left hand margin: oxidation number of vanadium. Limiting chemical shifts are indicated for organic (upper margin) and inorganic compounds (lower margin). *Abbreviations*: L = phosphine (mostly), isonitrile, amine, and others; Cp = η^5-cyclopentadienyl; Cp′ = Cp derivative; X = halide, hydride, OR, and others; E = group-16 donor; R = alkyl or aryl. The notation {} indicates the compound's core.

The standard commonly employed in ^{51}V NMR is neat $VOCl_3$. Since this is rather an aggressive compound which has to be handled sealed under inert gas atmosphere, aqueous solutions of 1 M sodium orthovanadate may be employed as a secondary standard. At a pH of 12, this solution contains two species, viz. $[VO_4]^{3-}$ ($\delta = -535.7$ relative to $VOCl_3$) and $[V_2O_7]^{4-}$ ($\delta = 559.0$). Since the chemical shifts of vanadium compounds are temperature dependent (in particular this applies to low-valent – and hence to many organovanadium – compounds), concentration, counter-ion and solvent dependent, it is imperative that comparison of ^{51}V chemical shift values within small shift ranges affords comparable temperature and environmental conditions. The solvent effects include solvent isotope effects, in particular so for polar solvents [4a] (Table 2).

In Section 2, a brief overview of the background of the main isotropic NMR parameters will be introduced, including phenomenological aspects. This section is not meant to provide a comprehensive treatise of the underlying theory. Rather, it is supposed to furnish some of the aspects necessary to interpret trends in NMR parameters. The discussions in Sections 3 and 4 will fall back hereunto.

2. NMR parameters

2.1. Shielding

Fig. 1 clearly shows that, within a family of compounds, shielding can vary dramatically. In particular, there is no obvious correlation between the oxidation state of vanadium and shielding: The shielding range for cyclopentadienylvanadium(III) complexes, e.g., overlaps with those for V^{-I}, V^{+I} and V^{V} complexes; and the distinct deshielding of the dinuclear vanadium(IV) complexes of general composition $\{(CpV)_2(\mu\text{-}E)_n\}$, where E is a bridging chalcogenide or dichalcogenide, rather is a consequence of the softness of these donors than of the high oxidation state of the central metal. Overall shielding σ is

a composite of three contributions, the local diamagnetic term, the local paramagnetic term and a non-local term:

$$\sigma = \sigma_{\text{local}}(\text{dia}) + \sigma_{\text{local}}(\text{para}) + \sigma_{\text{non-local}} \quad (1)$$

The non-local term is usually (i.e. in the absence of contact contributions stemming from paramagnetic constituents in the sample) small, giving rise to variations of several ppm in response to medium effects such as the polarity of the solvent, the nature of the counter-ion in the case of ionic compounds, and intermolecular interactions. The solvent isotope effect mentioned above (Table 2) is a non-local contribution. When discussing trends in chemical shifts related to variations in the first (and second) coordination sphere, $\sigma_{\text{non-local}}$ is commonly neglected. The local diamagnetic term essentially depends on the core electrons and thus, although sizable, is constant and hence again neglected in discussing shielding trends. Remains the paramagnetic term which, in a practicable version of Ramsey's treatment, employed in this review, can be represented by the following equation:

$$\sigma_{\text{local}}(\text{para}) = \frac{-e^2}{2mc^2}({}^1\Delta E^{-1})_{\text{av}}\left\langle r^{-3}\right\rangle_{3\text{d}} c^2 \quad (2)$$

The quantities $(\Delta E^{-1})_{\text{av}}$ (ΔE_{av} = average HOMO-LUMO splitting; only singlet transitions are allowed), $\langle r^{-3}\rangle_{3\text{d}}$ (r = distance of the 3d electrons) and c^2 (c = valence-d electron LCAO coefficient) correspondingly correlate with the ligand field strength, the nephelauxetic effect ("hard" vs. "soft" ligands), and the covalency of the metal–ligand bond; $c = 1$ in the crystal-field approximation. Note that σ_{local}(para) is a negative (deshielding) contribution, i.e. overall shielding σ decreases as σ(para) increases.

The factors influencing shielding are complex. Both, the σ donor and (in low-valent complexes) π acceptor strengths of the ligand are operative (mainly via ΔE and c), as is the nephelauxetic effect (mainly via r and c). In addition, the local symmetry of the complex comes in. The influence of symmetry arises from the selection rules for electronic transitions between lowest occupied and highest unoccupied levels, restricting allowed excitations to those molecular orbitals which have the same transformation properties as the angular momentum operator. Despite this complexity, the following empirical trends for shielding can be expected by considering Eq. (2).

2.1.1. Low-valent (closed-shell: d^8 (V^{-III}), d^6 (V^{-I}), d^4 (CpV^{+I}))

(1) An increase of ligand strength goes along with an increase in ΔE, a decrease of σ(para) and thus a relative increase of overall shielding σ. In low-valent complexes, effective π acceptors (such as carbonyl, phosphites and phosphines) are strong ligands, while effective σ/π donors are weak ligands. The latter category is represented by donor functions with low polarizability and high electronegativity χ of the donating function. The increase of shielding with decreasing χ is referred to as "normal electronegativity dependence of shielding". An example is the following series of pentacarbonylvanadates(−I) $[V(CO)_5L]^-$ of local C_{4v} symmetry (data from Ref. [4b]):

L = PF_3	$P(OMe)_3$	CNCy	PMe_3	$P(tBu)_3$	NCMe	$NHEt_2$	THF
−1961	−1928	−1901	−1875	−1833	−1601	−1498	−1367

Bulky ligands are less strong than comparable ligands of smaller size, and thus are weaker. Cf., e.g., PMe_3 and $P(tBu)_3$ in the above series.

(2) Highly polarizable ("soft") ligands give rise to comparatively small LCAO coefficients c and expand the 3d cloud, i.e. reduce $\langle r^{-3}\rangle_{3\text{d}}$. Both effects reduce contributions due to σ_{local}(para) and thus increase σ ("normal polarizability effect").

(3) In chelate complexes, ring strains, e.g., four-ring versus five-ring structures, or torsional strains in (6- and seven-membered ring systems) lead to an effective reduction of shielding, e.g., in the carbonylcyclopentadienylvanadium(+I) complexes $CpV(CO)_2\{Ph_2P(CH_2)_nPPh_2\}$: $n = 1$ (−870), $n = 2$ (−1110), $n = 4$ (−826).

2.1.2. High-valent (open shell: d^0 (CpV^{+V}), d^1 (spin-coupled dinuclear $\{CpV^{IV}\}_2$))

In complexes containing vanadium in a high valence state, strong ligands are represented by effective σ/π donors, i.e. "hard" ligands with high electronegativities. These ligands, usually coordinating via an *O*- or *N*-function, induce high overall shielding ("inverse electronegativity dependence"). Less electronegative and more polarizable ligands, such as bromide, iodide, sulfide, selenide and telluride, give rise to a pronounced deshielding, as shown for the following series of $CpV(NtBu)X_2$ (data from Ref. [5]; for the correlation between ^{51}V shielding and the ligand electronegativity see also Refs. [2,6]):

X = O*t*Bu	NH*t*Bu	SPh	Cl	Br	SePh	I	CH_3
−904	−894	−475	−457	−329	−304	−110	−25

Alkyl groups in these complexes have to be classified as weak and/or "soft" ligands.

The steric effects (bulky ligands; strains in chelate structures) are effective through changes in geometrical parameters, such as a prolongation of bond lengths and distortion of bond angles, both of which result in less effective overlap and thus less effective electronic interaction between ligand and vanadium. Changes in internuclear distances and angles also come about by variations in temperature, and by isotopic substitution in the ligand sphere. In the rovibrational frame [4,7], these influences can be related to variations of internal displacement coordinates Δr and, to a less pronounced extent, angular deformation $\Delta\alpha$. Increasing the temperature increases Δr and decreases shielding. For low-valent carbonylvanadium complexes, the temperature gradients are in the order of magnitude of −0.25 to −0.3 ppm/deg. ^{51}V shielding in high-valent vanadium complexes is sufficiently less sensitive to temperature changes. Deshielding of the ^{51}V nucleus is also observed for the lighter isotopomer (e.g., ^{12}CO or $C^{16}O$) as compared to the heavier isotopomer (e.g., ^{13}CO or $C^{18}O$). Alternatively, these effects can again be conceived on the basis of Eq. (2):

Increasing the temperature leads to an increase of the occupation of vibronically excited ground state levels, decreasing ΔE and σ_{para}, and increasing σ. Examples will be provided in the respective sections dealing with $[V(CO)_6]^-$ and $CpV(CO)_4$.

2.2. Nuclear spin–spin coupling

Nuclear spin–spin coupling (or scalar coupling) between a metal nucleus such as ^{51}V and a ligand nucleus in the *n*th coordination sphere, $^nJ_{VL}$, is dominated by the Fermi contact term as given by the following equation:

$$^nJ_{VL} = \text{const}\,(^3\Delta E^{-1})_{av}|S(0)_V|^2|S(0)_L|^2\sigma(s)^2 \quad (3)$$

The constant contains the magnetogyric ratios of the coupling nuclei. $(^3\Delta E)_{av}$ is the mean triplet excitation energy, $|S(0)_V|^2$ and $|S(0)_L|^2$ are the s-electron densities at the respective nuclei, and $\sigma(s)^2$ represents the σ(s) contributions to the V–L bond. Although π interactions do not explicitly appear in this expression, *J* is also substantially influenced by the extent of π-bonding (π donation in high-valent, back-bonding in low-valent complexes) via the σ–π synergism. As a consequence, effectively σ- and π-interacting ligands can give rise to sizable couplings. The coupling constants rapidly decrease as the distance between the coupling nuclei increases, i.e. two-bond coupling ($n=2$) is rarely observed. But even the observability of one-bond coupling ($n=1$) is often unresolved due to broad resonance lines. Since, as elucidated in Section 2.3, broad lines go along with effective (i.e. fast) relaxation, the absence of coupling may also come about through relaxation decoupling.

2.3. Relaxation (line widths)

Relaxation is particularly effective for quadrupolar nuclei. The dominating mechanism here, the quadrupole mechanism, has its origin in fast energy transfer from the excited nucleus to its environment. This energy transfer is imparted by the interaction of the nuclear electric field gradient (a tensor) and inhomogenous electric fields produced by tumbling dipoles. In systems dominated by quadrupole relaxation, the "energetic" and "entropic" relaxation times T_1 and T_2, respectively, are about equal in the extreme narrowing regime (i.e. sufficiently fast tumbling of the molecule under consideration). The relaxation time *T* is inversely proportional to the line width, commonly quoted as the width of the resonance signal at half height, $W_{1/2}$:

$$W_{1/2}(^{51}V) = (\pi T)^{-1} = 0.041\pi^2 C_Q \left(\frac{1+\eta^2}{3}\right)\tau_c \quad (4)$$

Here, $C_Q = e^2 q_{zz} Q/h$ is the nuclear quadrupole coupling constant (q_{zz} = electric field gradient in *z*-direction, *Q* = nuclear quadrupole moment (Table 1)), η is the asymmetry parameter and describes the deviation from cylindrical symmetry (for cylindrical symmetry, $\eta=0$), and τ_c, the molecular correlation time, describes the molecular tumbling and thus becomes a measure for the interaction between solvent and solute molecules. According to Eq. (4), broad lines are to expected for:

- large molecules and molecules containing bulky ligands (slow tumbling);
- high viscosity accompanying high concentration, low temperature (slow tumbling) and polar solvents;
- low point symmetry (sizable *q* and η).

As already mentioned in Section 1, the $Q(^{51}V)$ is comparatively small, and spectra are usually well resolved. Particularly narrow lines are observed under cubic symmetry and in certain cases of C_{nv} symmetry, e.g., *fac*-$[VL_3(L')_3]$: C_{3v}; $CpV(CO)_4$: C_{4v}. Comparatively sharp resonance signals are also observed in the presence of strong π-accepting ligands (low-valent vanadium) or strong σ/π-donating ligands (high-valent vanadium).

3. NMR data

3.1. Alkyl, aryl, alkylidene and alkylidyne complexes

While alkyls and aryls coordinate to vanadium via a σ-bond, alkylidenes (carbenes) and alkylidynes (carbynes), L, additionally interact through one or two π bonds, which can either be L → V donor bonds (high-valent vanadium) or L ← M acceptor bonds (π back donation; low-valent vanadium). The latter situation resembles the ligand-to-vanadium interaction in carbonyl and isonitrile complexes; these ligands will, however, be treated separately in Section 3.2.

Vanadium NMR spectroscopic data are available for alkylvanadium complexes containing vanadium in the oxidation states +V, +IV and +I. The vanadium(V) compounds are represented by two families: (i) $E{=}VR_nX_{3-n}$ (E = O or NR, X = Hal, OR or NR_2), and (ii) $CpV(=E)R_nX_{2-n}$.[1] For the complexes of the general composition $E{=}VR_nX_{3-n}$, Scheme 1, the following trends can be noted: (1) with increasing number of alkyl groups attached to the V=NR or V=O moiety, shielding decreases, classifying alkyls – as already noted in Section 2.1 – as weak/soft ligands; cf. **1a** to **1d** [8] and **4a** to **4d** [9]; (2) with increasing bulkiness of the alkyl group shielding increases (**5**) [10]; (3) replacing neopentyl for (trimethylsilyl)methyl (**1a/2a**) [11a] accounts for a negligible change only; (4) if, however, NR_2 (**1b**) is replaced by OR (**3**) [11b], the ^{51}V nucleus is deshielded, as expected, since the amide substituent is less electronegative than alkoxide. This effect is also obvious for compounds **6a/6b** [12], but it is reversed in the cyclopentadienyl complexes **7a/7b** [6] (Scheme 2); (5) somewhat surprisingly, a sizable down-field shift of 169 ppm is also observed for a second-sphere substituent effect, i.e. on going from N*t*Bu (**2a**) to NTol (Tol = toluenyl, **2b**) [13]. A second-sphere effect has also been noted for the adduct formed between **4a** and tris(trimethylsilyl)aluminium, $(CH_2SiMe_3)_3Al{\cdot}$**4a** [9]. Shielding is reduced from +1205 (**4a**) to +1575 (for the adduct with the aluminium alkyl), suggesting association of the aluminium alkyl via the doubly bonded

[1] The bond between V and E (O or NR) will be considered as a double bond (V=O, V=NR) throughout this review, i.e. in terms of a σ-donor + π-donor bond. Alternatively, the bonding situation can be (and has been) treated in terms of a triple bond (V≡O, V≡NR; σ-donor plus two π-donor bonds).

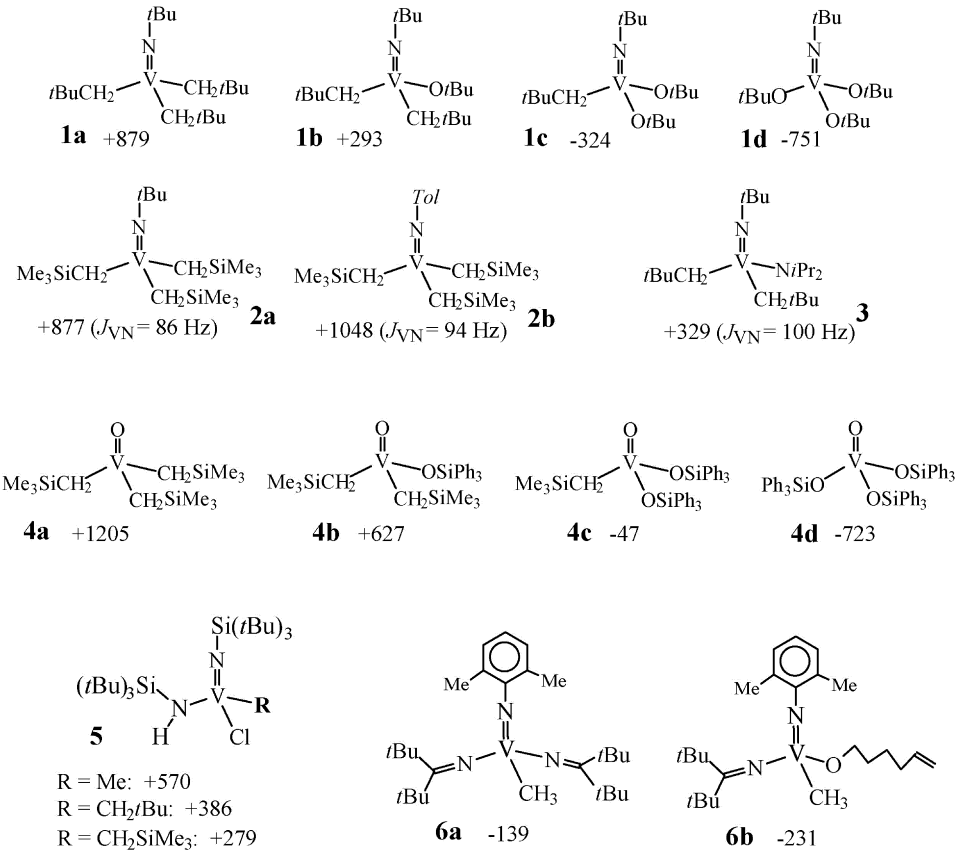

Scheme 1.

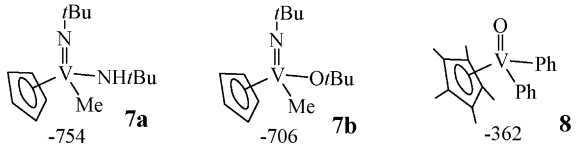

Scheme 2.

oxo group, thus diminishing the donating power/reducing the effective electronegativity of the oxo group. This topic will be resumed in the context of ethylene polymerization in Section 4. The introduction of the η^5-cyclopentadienyl ligand, **7** [6] and **8** [14] in Scheme 2, drastically increases shielding in comparison to, e.g., the complex series **1** and **4**.

Line widths $W_{1/2}$ very much reflect the symmetry: while $W_{1/2}$ values for **4a** and **4d** (local C_{3v} symmetry) are 50 and 100 Hz, the respective values for **4b** and **4c** (C_{2v}) are 500 and 400 Hz. In the complexes **5**, line widths decrease with increasing bulk of R (R = Me: $W_{1/2}$ = 230, R = CH$_2$*t*Bu: $W_{1/2}$ = 180, R = CH$_2$SiMe$_3$: $W_{1/2}$ = 150 Hz), contrasting what one would expect in terms of molecular correlation (Eq. (4) in Section 2.3), and thus apparently reflecting influences rooting in nuclear quadrupole coupling. Note that in three cases, **2a**, **2b** and **3**, $^1J(^{51}V–^{14}N)$ is resolved.

The shielding in compounds **9** (−3) and **10** (−1 ppm) [10], Scheme 3, containing a four-membered cyclic system (vanada-azacyclobutane and -butene, respectively) and just one vanadium–carbon bond may be compared with **6a** (−139, Scheme 1), containing the same donor set, RN=VN$_2$C. The higher shielding in **9** and **10** may reflect a more efficient vanadium–Cσ interaction in the fixed ring structure. Compound **11** [15a] represents a rare example of a carbon-to-vanadium triple bond ($\sigma + 2\pi$), with the alkylidyne (carbyne) ligand giving rise to a particularly high shielding, −956, exceeding that of inorganic vanadium(V) compounds (VF$_5$, −895). High shielding has also been noted for the neutral variant of **11** (with

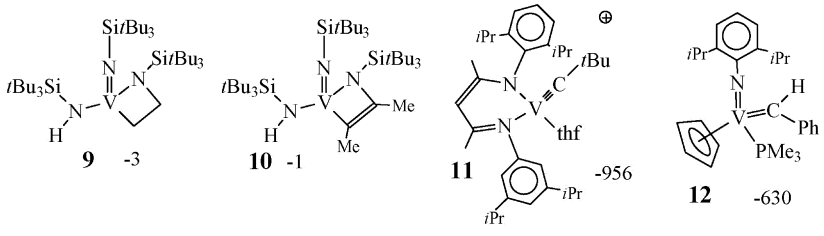

Scheme 3.

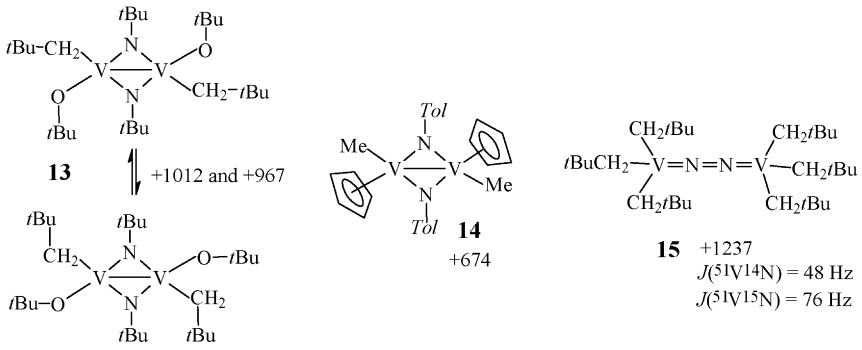

Scheme 4.

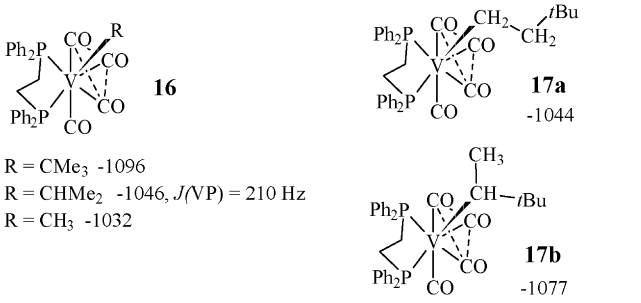

Scheme 5.

teflate instead of thf; −882 ppm), and further, although not to that extent, for the alkylidene (carbene) complex **12** (−630) [15b] and for alkenes coordinating in the side-on mode (Section 3.2).

Mononuclear vanadium(IV) complexes (d^1) are paramagnetic and thus NMR silent. In dinuclear complexes with strong electronic coupling, ^{51}V NMR resonances are observed which again fall into the low shielding range. Two examples are depicted in Scheme 4. In both complexes, **12** [16] and **13** [17], there is an identical $\{V_2(\mu\text{-}NR)_2\}$ core. For complex **12**, two signals have been observed in a 1:1 ratio at 293 K, assigned to two rotamers in comparatively slow equilibrium. Complex **14** contains two tris(neopentyl)vanadium units linked by dinitrogen [18]. Depending on whether the $\{N_2\}$ moiety is taken as neutral dinitrogen or as diazenido(2-), vanadium is in the oxidation state +III (d^2) or +IV (d^1). In the former case, a low spin configuration is necessary to provide diamagnetism, which is not easily envisaged in tetrahedral V^{III} environments. ^{51}V NMR thus supports the assignment $(V^{IV})_2(\mu$-diazenido(2-), presupposing strong antiferromagnetic coupling between the two V^{IV} centres. This view is corroborated by the N–N bond length (corresponding to a double bond) determined by X-ray diffraction. The ^{51}V NMR of ^{14}N-**14** shows a quintet with a coupling constant $^1J(^{51}V–^{14}N) = 48$ Hz. In ^{15}N-**14**, the expected virtual triplet is observed; $^1J(^{51}V–^{15}N) = 76$ Hz. The larger coupling constant for the ^{15}N variant reflects the larger magnetogyric ratio of ^{15}N.

Low-valent vanadium complexes with alkyl and alkylidene ligands, for which ^{51}V NMR data have been reported, belong to the family $RV(CO)_4$dppe (V^{+I}, dppe = $Ph_2PCH_2CH_2PPh_2$), with R capping a face of an octahedral $\{V(CO)_4$dppe$\}$ core. The compounds, which are synthesised from anionic precursors $[V(CO)_4$dppe$]^-$ and RI, or by hydrovanadation of alkenes (to yield alkyl complexes; **16** and **17** in Scheme 5) or alkynes (to yield the *Z*-alkynyl complexes; **18**), cover a comparatively narrow range of chemical shifts (ca. −1010 to −1100). They thus exhibit high-field shifts with respect to practically all of the alkyl complexes introduced so far. They are, however, deshielded with respect to the octahedral V^{-I} precursors ($[V(CO)_4$dppe$]^-$: −1790) and the hepta-coordinated, face-capped octahedral hydridovanadium precursors ($HV(CO)_4$dppe: −1690). In the case of the alkyl complexes **17**, the anti-Markovnikov adduct is obtained as the main product (**17a**) along with minor amounts of the Markovnikov adduct (**17b**) with no substantial differences in the chemical shifts.

3.2. Side-on coordinating ligands

In this section, ligands coordinating in the η^2 mode such as alkenes, alkynes, acyl and carbon disulfide will be addressed,[2] along with η^3-allyl complexes. The complexes are depicted in Scheme 6.

Alkene and/or alkyne complexes are known for vanadium in the oxidation states −I, +I, +III and +V. Complexes **19**, **20** and **21** [20] derive from $[V(CO)_6]^-$ by photo-induced substitution of one carbonyl. They are stable in organic solvents

[2] The η^2-bonding mode can be described by a resonance hybrid. In this description, one of the limiting structures is the neutral ligand, interacting through its π system (σ donor bond(s)) and its π* system (π back bond). This is the structure variant employed in this review throughout. The second limiting structure is the dianionic ligand binding in a "butterfly"-like manner, i.e. forming two covalent C → V donor bonds, using sp^3 or sp^2 hybrid orbitals at the carbons.

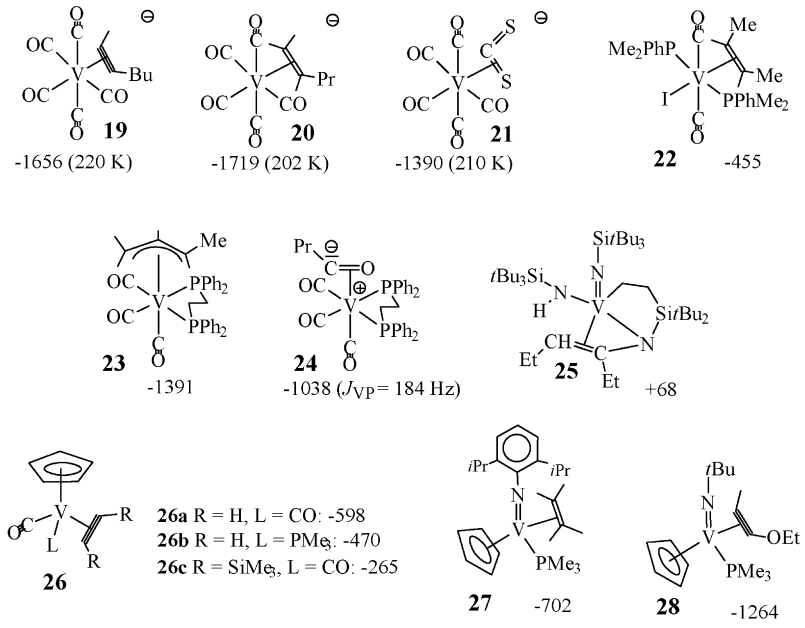

Scheme 6.

such as THF at low temperature only. For direct comparison with chemical shifts obtained at room temperature, the low temperature shifts can be extrapolated to 300 K, using a temperature gradient of −0.25 ppm per degree as noted in Section 2.1 and discussed in more detail in the next section (Section 3.3). One then arrives at $\delta_{300} = -1636$ (complex **19**), −1695 (**20**) and −1368 (**21**), i.e. substantial deshielding with respect to hexacarbonylvanadate(−I) (−1955), mainly reflecting the less efficient bonding interaction with the η^2-π ligands when compared to CO. Still more pronounced is deshielding in the iodovanadium(+I) complex **22** [21], where replacement of two additional carbonyls by phosphines adds to the deshielding. In the tri-carbonylvanadium(+I) complexes **23** (with a η^3-allyl(1-) ligand [22]) and **24** (with a η^2-acyl(1-) ligand [23]), shielding is in-between the pentacarbonyl and dicarbonyl species. The vanadium(V) complex **25** [10], related to **9** and **10** in Scheme 3, falls within the shielding range for this type of complexes.

Deshielding on substituting carbonyl for alkyne/alkene in carbonylvanadium(−I and +I) complexes is also pronounced in complex **26** [24], a derivative of η^5-CpV(CO)$_4$ ($\delta = -1533$). As obvious from electron counting, the alkyne acts here as a four-electron donor, but cannot compete in ligand strength with two carbonyls. Interestingly, the bis(silyl)alkyne in **26c** is even less strong than alkyne (**26a**) itself. As will be discussed in more detail in Section 3.3, phosphines are also weaker than CO (**26b** vs. **26a**). For the complex **27** [15b], with V^{III} (or V^{V} if the alkene is considered to coordinate in the 'butterfly' mode; cf. footnote 2), a shielding situation arises which is similar to that in the related complexes **7** and **8** (Scheme 2). The reason for the substantially more pronounced shielding in the very similar alkyne complex **28** [25] remains elusive.

The dinuclear μ,η^5:η^3-cyclooctatetraene(2-) complex **29** in Scheme 7 with a formal triple bond ($\sigma^2\pi^2\delta^2$) between the two V^{III} centres exhibits a chemical shift of +1140 ppm

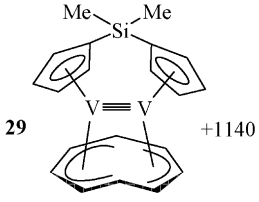

Scheme 7.

(at 298 K, +1283 at 200 K)) [26]. When compared with the organovanadium complexes in Scheme 6, the ^{51}V nucleus in **7** is remarkably deshielded, reminiscent of similar features in vanadium coordination compounds with non-innocent ligands (such as catecholates and hydroxamates), i.e. ligands which are able to effectively delocalize electron density towards vanadium. In addition to the particularly low shielding, the large temperature gradient of −1.5 ppm/deg is noteworthy.

3.3. Carbonyl and isonitrile

While carbonylvanadium complexes are restricted to low-valent vanadium (in the diamagnetic states V^{-III}, V^{-I}, V^{+I}), isonitriles can stabilise low and high-valent vanadium. The carbonylvanadates $[V(CO)_5]^-$ (−1965), $[V(CO)_6]^-$ (−1955) and the trifluorophosphine derivatives of the latter ($[V(CO)_{6-n}(PF_3)_n]^-$, e.g., *fac*-$[V(CO)_3(PF_3)_3]^-$; $\delta = -1964$) mark the high-field margin of shielding in this family of complexes. PF_3 matches CO in strength. Fig. 2 illustrates the ^{51}V NMR spectrum of a mixture of $[V(CO)_{6-n}(PF_3)_n]^-$ complexes. An even more effective shielding is induced by triphenylstannyl(1-); the dianion $[V(CO)_5SnPh_3]^{2-}$ has a chemical shift −1994. The high shielding in this case is due to the high polarizability (softness) of the ligand, reducing the factor $\langle r^{-3}\rangle c^2$ in Eq. (2). Any other ligand substituting CO in $[V(CO)_6]^-$ leads to deshielding, which is particularly

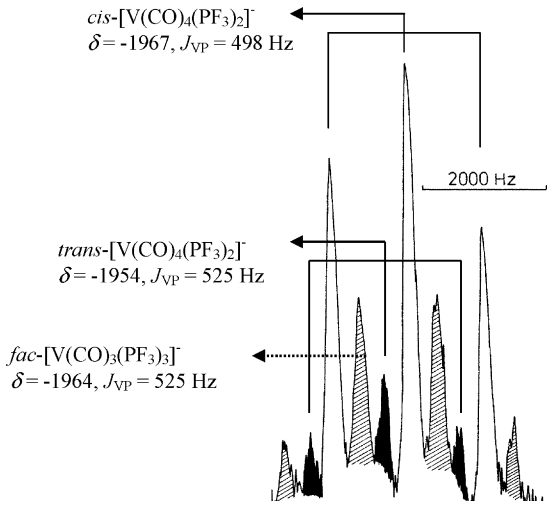

Fig. 2. ^{51}V NMR spectrum of a mixture of $[Et_4N][V(CO)_{6-n}(PF_3)_n]$ ($n = 2$ and 3) in THF, showing the superimposed triplets for $n = 2$ plus quartet for $n = 3$. Data from Ref. [5].

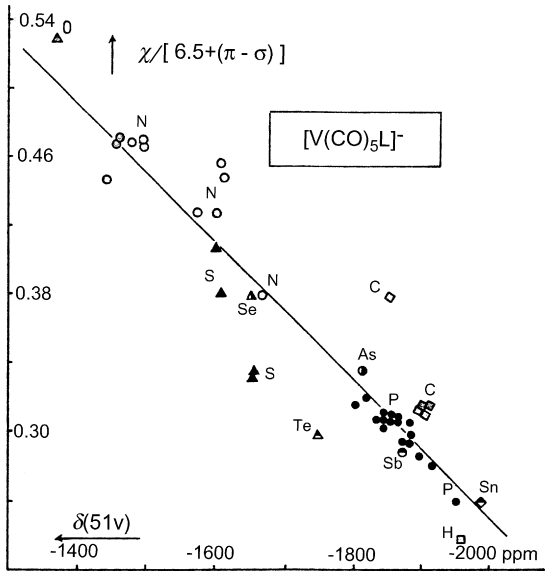

Fig. 4. The plot of chemical shifts (extrapolated to 300 K where necessary) for the anions $[V(CO)_5L]^-$ vs. $\chi \times [6.5 + (\pi + \sigma)]^{-1}$ (see text for the empirical parameters) represents the about linear relationship between shielding δ and ΔE^{-1} to be expected from Eq. (2). Reprinted (slightly modified) with permission from Ref. [20b]. ©American Chemical Society.

pronounced for weak ligands (weak in low-valent vanadium compounds) such as *O*- and *S*-functional donors. Fig. 3 provides an overview for $[V(CO)_5L]^{n-}$ complexes [20b], where L is a group-14, -15 or -16 donor ligand. Additional examples for $L = PZ_3$ are collated in Table 3. Accordingly, phosphites ($Z = OR$) are stronger ligands than phosphines ($Z = R$). Increasing bulk of R and thus steric demand of PR_3, as quantified by, e.g., the cone angle, also causes a deshielding effect. Further, shielding decreases with increasing substitution of CO for PR_3. In the anions $[V(CO)_4PP]^-$ (PP is a bidentate phosphine ligand), the ring size also plays a role [27a] (cf. also Section 2.1).

Table 3
^{51}V chemical shifts of phosphine derivatives of hexacarbonylvanadate(−I)

$[V(CO)_5PZ_3]^-$	δ ($^1J_{VP}$, Hz)	$[V(CO)_4(PP)]^-$	δ
$PZ_3 = PF_3$	−1961 (488)	$PP = Ph_2PCH_2PPh_2$	−1590
$PZ_3 = P(OMe)_3$	−1928 (366)	$PP = Ph_2P(CH_2)_2PPh_2$	−1790
$PZ_3 = PMe_3$	−1875 (214)	$PP = Ph_2PCH{=}CHPPh_2$	−1830
$PZ_3 = P(tBu)_3$	−1833 (210)	$PP = Ph_2P(CH_2)_3PPh_2$	−1723
$PZ_3 = PPh_3$	−1813 (204)	$PP = Ph_2P(CH_2)_4PPh_2$	−1699
$PZ_3 = P(NEt_2)_3$	−1806 (293)	$[V(CO)_3triphos]^-$ [a]	−1720

Data from Refs. [5,27].
[a] triphos = $Ph_2P(CH_2)_2PPh(CH_2)_2PPh_2$.

The relationship between shielding and factors influencing the electronic situation as described by Eq. (2), and reflected qualitatively in Fig. 3 for $[V(CO)_5L]^-$, can be quantified as depicted in Fig. 4. Here the chemical shift is plotted against the quantity $\chi \times [6.5 + (\pi + \sigma)]^{-1}$ [20b], in which χ stands for the Pauling electronegativity of the donating function of the ligand L. The values π and σ are Graham's IR-spectroscopic parameters, calculated from the CO force constants, and quoted relative to $[V(CO)_5NEt_3]^-$ ($\pi = 0$, $\sigma = 0$, $\delta = -1456$). The value

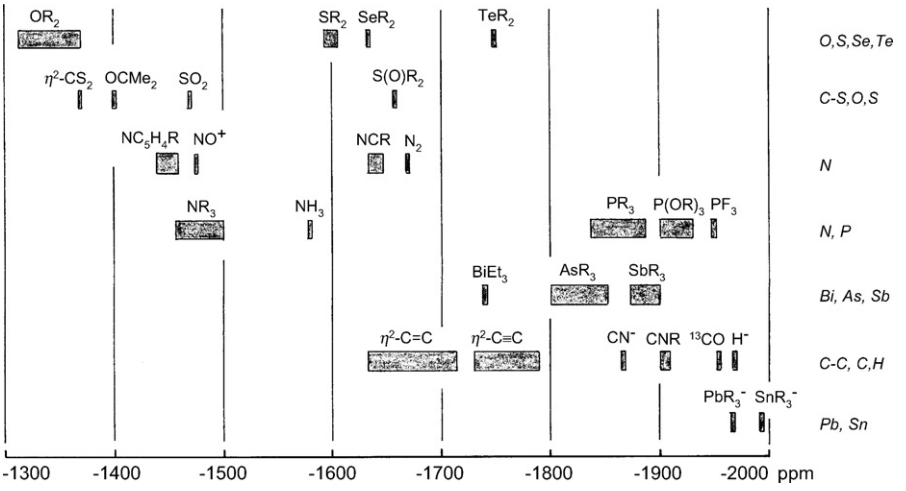

Fig. 3. Chemical shift ranges for $[V(CO)_5L]^{n-}$ complexes; for the donor functions, see the right hand margin. Chemical shifts [27] are quoted relative to $\delta(VOCl_3) = 0$.

Table 4
^{51}V chemical shifts for octahedral (left) and face-capped trigonal-prismatic (right) carbonylvanadium(I) complexes

Complex	δ	Ref.	Complex	δ	Ref.
$[V(CO)_5NO]$	−1489	[28a]	$[HV(CO)_4dppe]$[a]	−1690	[28b]
$[V(CO)_4NO(PMe_3)]$	−1460	[28a]	$[IV(CO)_4dppe]$	−1706	[19b]
$[V(CO)_4NO(dppe)]$	−1379	[28b]	$[BrV(CO)_4dppe]$	−1698	[19b]
			$[BrV(CO)_4(dmpe)]$[b]	−1804 (J_{VP} 152 Hz)	[19b]
$[(Ph_3PAu)V(CO)_5]$	−1836	[29]	$[BrV(CO)_2(dmpe)_2]$	−859 (J_{VP} 159 Hz)	[19b]

[a] dppe = $Ph_2P(CH_2)_2PPh_2$.
[b] dmpe = $Me_2P(CH_2)_2Me_2$.

Table 5
One-bond ($^1\Delta(^{13}CO)$, $^1\Delta(^2H)$) and two-bond ($^2\Delta(C^{18}O)$, $^2\Delta(^2H)$) isotope shifts for $[V(CO)_6]^-$ and carbonyl-halfsandwich complexes

$[V(CO)_{6-n}(^{13}CO)_n]^-$	$^1\Delta(^{13}CO) = -0.27$	$[V(CO)_{6-n}(C^{18}O)_n]^-$	$^2\Delta(C^{18}O) = -0.10$
$C_5H_5V(CO)_{4-n}(^{13}CO)_n$	$^1\Delta(^{13}CO) = -0.46$	$C_5H_5V(CO)_{4-n}(C^{18}O)_n$	$^2\Delta(C^{18}O) = -0.1$
$C_5Me_5V(CO)_{4-n}(^{13}CO)_n$	$^1\Delta(^{13}CO) = -0.42$	$[C_5H_5V(CO)_3{}^2H]^-$	$^1\Delta(^2H) = -0.46$
$C_7H_7V(CO)_{3-n}(^{13}CO)_n$	$^1\Delta(^{13}CO) = -0.38$	$C_5H_{5-n}(^2H)_nV(CO)_4$	$^2\Delta(^2H) = -0.72$

Mean values per isotopic substitution are given. Data from Refs. [4,7,30].

6.5 is a correction factor, accounting for the arbitrary assumption of NEt_3 having zero σ donor and π acceptor power. This quantity $\chi \times [6.5 + (\pi + \sigma)]^{-1}$, which contains empirical parameters only, takes the place of the term $(\Delta E^{-1})\langle r^{-3}\rangle c^2$ in Eq. (2).

DFT calculations on $[V(CO)_6]^-$ and $[V(CO)_5N_2]^-$ have provided satisfactory agreement between calculated and experimental chemical shift values [28]:

	$\lvert\delta_{calcd}\rvert$	$\lvert\delta_{exp}\rvert$
$[V(CO)_6]^-$	2090	1955
$[V(CO)_5N_2]^-$	1847	1671

The nitrosyl ligand NO^+ also induces substantial deshielding ($[V(CO)_5NO]$: $\delta = -1460$ at 245 K). Further, the ^{51}V nucleus is less shielded in carbonylvanadium(+I) than in carbonylvanadates(−I), comparable ligand sets provided. In Table 4, data for selected examples of V^{+I} complexes derived from $[XV(CO)_6]$ (X = hydride or halide) are listed.

In the complex anions $[V(CO)_5PZ_3]^-$ not only shielding, but also vanadium–phosphorus coupling is subject to the nature of Z. The size of the one-bond coupling constants $^1J_{VP}$ correlates with the electronegativity of Z and thus indirectly with the π acceptor power of PZ_3. As stated in Section 2.2, effectively π-accepting ligands (such as PF_3 and phosphites and, to a certain extent, also phosphines with a small cone angle such as PMe_3) synergistically enhance the σ_s-electron density at the coupling nuclei (the $|S(0)|^2$ terms in Eq. (3)), which causes increased coupling interaction. Vanadium–phosphorus coupling is not always resolved, because of broad resonance lines. The larger and the less symmetric the system, the broader are the signals, in accordance with Eq. (4) in Section 2.3. A decrease in temperature also increases line widths because of a gain in viscosity. This is shown in Fig. 5, left, for Z = *p*-fluorophenyl: coupling brakes down at about 240 K.

Fig. 5, right, illustrates the upfield shift for $[V(CO)_6]^-$ as the temperature decreases. The rovibrational approach (Sec-

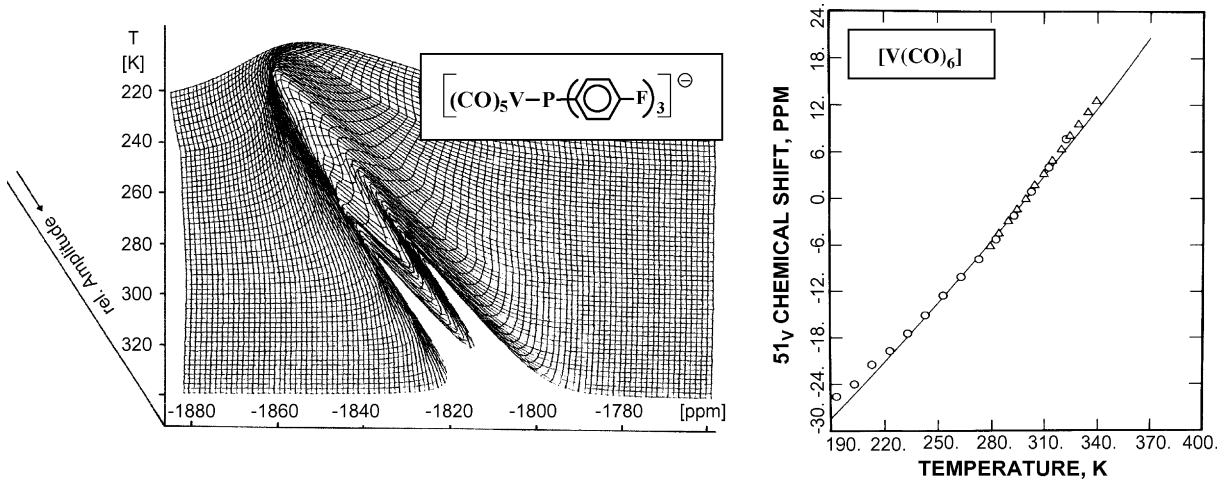

Fig. 5. Left: temperature-dependent ^{51}V NMR spectra of $[Et_4N][V(CO)_5PR_3]$ (R = *p*-fluorophenyl), 0.18 M in THF. On decreasing the temperature, shielding increases and line widths increase. In the temperature range of 320 to ca. 260 K, vanadium–phosphorus coupling is resolved (J_{VP} = 240 Hz); at lower temperature, relaxation decoupling occurs. Right: observed temperature dependence of shielding for $M[V(CO)_6]$, M = $[Et_4N]$ (◯) and $[Na(diglyme)_2]$ (△). The solid line represents the calculated temperature dependence. The shift scale (ordinate) is relative to $[V(CO)_6]^-$ at 298 K; $\delta = 0$ (−1955 relative to $VOCl_3$). Right part of the figure reprinted with permission from Ref. [7]. ©American Chemical Society.

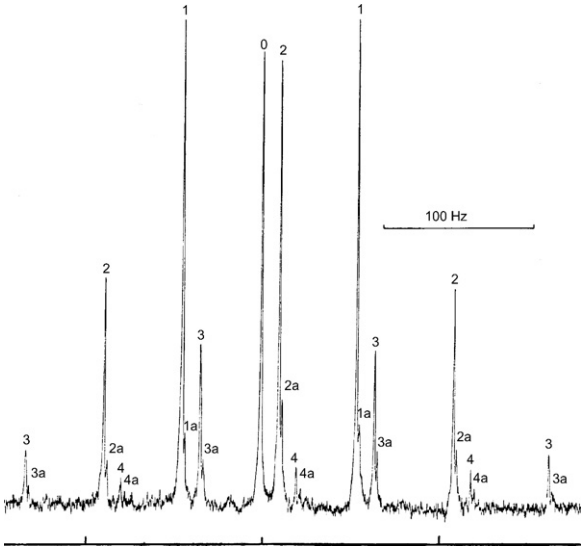

Fig. 6. 23.66 MHz ^{51}V NMR spectrum of $[V(CO)_{6-n}(^{13}CO)_n]^-$ [30b]; the degree of enrichment is 26%; scale division 5 ppm. The isotopomers for $n = 0$–4 can be identified and assigned to the respective multiplets ($^1J(^{51}V–^{13}C) = 116.1$ Hz). As an example, the centre for the $[V(CO)_4(^{13}CO)_2]^-$ triplet, $n = 2$, is shifted to high field with respect to $[V(CO)_6]^-$, $n = 0$. Minor isomers (*cis* and *trans*, *mer* and *fac*) are labelled 2a, 3a and 4a.

tion 2.1) to quantify this temperature effect (solid line) is compared with the experimental values (symbols). Experimental and calculated values form an about straight line with a slope (temperature gradient, tg) of −0.30 per degree. Similar tg's have been noted for pentacarbonyl-phosphinevanadates [7]. The closely related isotope effect (increase of shielding for the heavier isotope) is shown in Fig. 6; data are provided in Table 5.

Complexes containing the isonitrile ligand CNR (for data see Table 6) reflect similar shielding conditions. CNR is isoelectronic with CO. The chemical shift for $[V(CO)_5CNR]^-$ (−1908) and $CpV(CO)_3(CNR)$ (−1403 to −1407) [31] classifies isonitriles as rather strong ligands, comparable in strength with phosphites and small trialkylphosphines. Trends are comparable to those discussed for carbonyl complexes.

3.4. Aromatic and related ligands

The most prominent aromatic ligand coordinating to vanadium is η^5-cyclopentadienyl, Cp, and its derivatives; see also the previous sections, where Cp complexes have been dealt with in the context of the additional ligands in the ligand sphere. Most of the NMR data available are on $CpV(CO)_4$ and its substitution products (i) in the carbonyl sphere and (ii) at the Cp ring. Substitution in the carbonyl sphere essentially follows the patterns discussed for derivatives of $[V(CO)_6]^-$ (Figs. 3 and 4 and Table 3) and $[XV(CO)_6]$ (Table 4), not unexpectedly since $CpV(CO)_4$ type complexes, with the electron configuration d^4, again represent closed-shell systems. The parent complex $CpV(CO)_4$ (**30** in Scheme 8) has a chemical shift of −1534, which is exceeded by the complexes $[CpV(CO)_3H]^-$ (−1730, **31**) and $[CpV(CO)_3SnPh_3]^-$ (−2054), the latter marking the high-field margin of ^{51}V chemical shifts [32]. Shielding increases by ca. 100 ppm with respect to $CpV(CO)_4$ in the dinuclear complex **32** (Scheme 8) and the cationic η^6-tolyl complex **33**, while deshielding of ca. 50 ppm is noted for the d^6 (V^{-I}) complex η^7-tropyliumvanadium(−I), **34** [32].

Ring anellation at cyclopentadiene(1-) also results in deshielding (**35** to **39** in Scheme 9), which is more pronounced for anellation of a six-ring (the indene complex **35**) than of a seven-ring (the azulene complex **37**), and for anellation of two instead of just one six-ring (**35** vs. the fluorene complex **36**) [32]. The dinuclear complexes **37** and **38** form by reaction of hexacarbonylvanadium and azulene [32] or acenaphthylene [33], respectively, accompanied by cylopentadienylization and reductive coupling of the organic ligands. For the azulene complexes, ortho–ortho (o–o), para–para and ortho–para coupling is principally possible, and the $\{V(CO)_4\}$ units can be arranged *endo* or *exo*. Further, the two sp^3-hybridized carbons are centres of chirality, and the Cp planes are enantiotopic. In Scheme 9, the o–o *exo* form for **37** is shown, in analogy to the acenaphthylene complex **38**, for which this arrangement has been verified by structure analysis. The 27 possible isomers of **37** can, in principle, give rise to 15 distinct NMR signals. Only 4 to 5 signals are, however, observed, two of which account for about 95% of

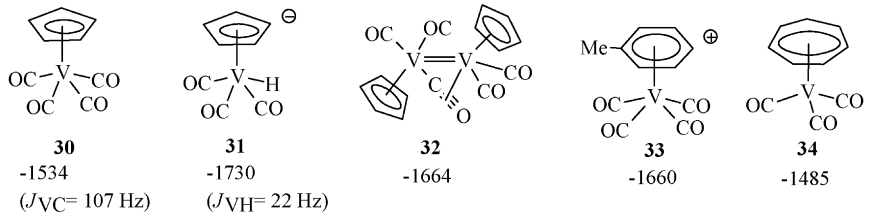

Scheme 8.

Table 6
Chemical shift data for isonitrile complexes

$[VX(NO)_2(CNiPr)_3]$	δ	Ref.		δ	Ref.
X = Cl	−847	[28b]	$CpV(CO)_3CNCy$	−1401	[31]
X = Br	−873	[28b]	$CpV(CO)_3CNBz$	−1407	[31]
X = I	−922	[28b]	$CpV(CO)_2(CNtBu)_2$	−1268	[31]
$[V(NO)_2(CNiPr)_4]I$	−1042	[28b]	$[V(CO)_5CNCy]^-$	−1908	[21]

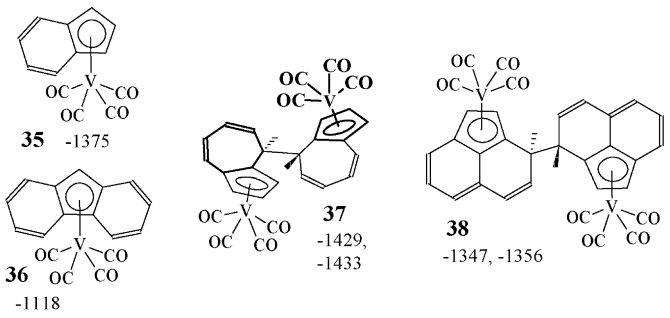

Scheme 9.

the overall intensity (Fig. 7, left). Similarly, complex **38** shows only two ^{51}V NMR signals in solution ($\Delta\delta = 9$ ppm), assigned to the *meso* forms resulting from the o–o *exo–exo* coupling.

Dissolved in mesophases such as Nematic Phase 4® (Merck), $CpV(CO)_4$ shows a first order quadrupole pattern consisting of the expected seven lines (Fig. 7, top right). The 1st order quadrupole splitting is 13.84 kHz, and the ordering factor S_a, estimated from the quadrupole coupling constant C_Q (2.8 MHz) and the quadrupole moment Q (-4.8 fm^2), is $S_a = 0.11$. The C_Q value and asymmetry parameter ($\eta = 0.11$) are obtained from an evaluation of the static solid state spectrum of polycrystalline $CpV(CO)_4$ (Fig. 7, bottom left), which shows a second order pattern, evidenced by the split central component flanked by two satellite lines [34].

The deshielding noted for $CpV(CO)_4$ on anellation in part reflects a ring substituent effect which is also pronounced as hydrogen atoms in C_5H_5(1-) are replaced by alkyl, functionalized alkyl and halide substituents [32,33,35,36]. A selection of data is provided in Table 7. Any substitution goes along with a deshielding, irrespective of the electronic substituent effects (M and I effects), suggesting that deshielding comes about by sterically disfavoured (with respect to the parent $CpV(CO)_4$) V–Cp′ interaction, where Cp′ stands for substituted Cp. This view is supported when comparing $(C_5H_4Me)V(CO)_4$ (-1525; $W_{1/2} = 43$ Hz) and $(C_5H_4trityl)V(CO)_4$ (-1484, $W_{1/2} = 350$ Hz) with substituents of comparable electronic behaviour. This steric influence also gives rise to an almost eightfold increase in line widths $W_{1/2}$ for these two compounds. Positional isomers of di- and tri-substituted species, e.g., $(1,2\text{-}C_5H_3Me_2)V(CO)_4$ and $(1,3\text{-}C_5H_3Me_2)V(CO)_4$ produce two separate signals, separated by 4–5 ppm. In the case of two unlike substituents, the Cp ring of the complex becomes enantiotopic (planar chirality, *p*). If one of the substituents contains a chiral centre, there are four diastereomeric combinations, and accordingly four signals are present [33]. The four diastereomers are shown for 1,2- and $\{1,3\text{-}C_5H_3Me(sBu)\}V(CO)_4$, **39**, in Scheme 10. The "two-bond" deuterium isotope effect in $\{C_5(^1H)_{5-n}(^2H)_n\}V(CO)_4$, -0.72 ppm per deuterium [4] (see also Table 5 in the previous section), is surprisingly large when compared with the one-bond effect of -0.54 in the anion $[CpV(CO)_3{}^2H]^-$, suggesting participation of orbitals associated with the C–H bonds in Cp–V bonding.

Fulvene complexes are related to cyclopentadienyl complexes, and can be represented by resonance hybrids as shown for the 6,6′-dithioethylenefulvene-V^{+I} complex **40** in Scheme 11, and the 6-dimethylaminofulvene-V^{-I} complex **41** [37]. Again, substitution, here at the Cp/fulvene ring *and* within the remaining ligand set reduces shielding. The two vanadium(II) centres in the dinuclear complexes **42** in Scheme 12, bridged by two

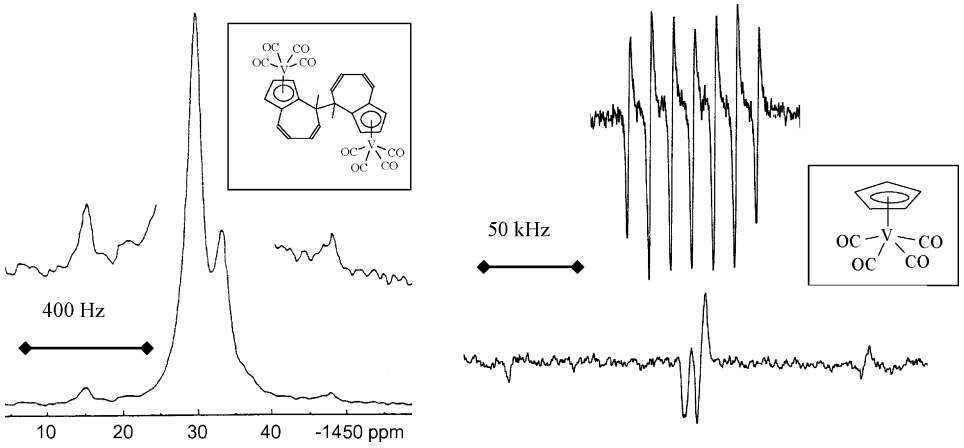

Fig. 7. Left: 78.94 MHz ^{51}V NMR spectrum of a $CDCl_3$ solution of $\{azuleneV(CO)_4\}_2$ (see also **37** in Scheme 8 for one of the isomers). Right: 16 MHz ^{51}V NMR spectra (1st derivatives) of $CpV(CO)_4$ in Nematic Phase 4 (top) and in the polycrystalline solid state (bottom) [34]. See text for discussion.

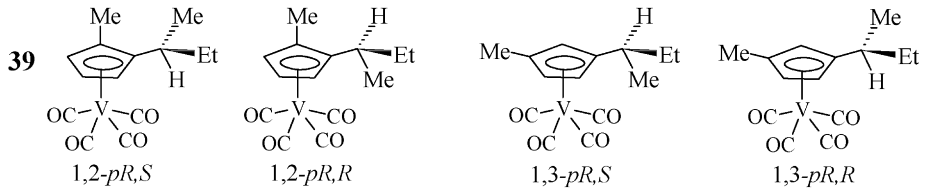

Scheme 10.

Table 7
Chemical shifts for derivatives of $CpV(CO)_4$ with ring substituents; references in square brackets

$C_5H_5V(CO)_4$	−1534 [32]	$C_5H_4R(CO)_4$	
$C_5H_4MeV(CO)_4$	−1525 [32]	R = Me	−1525 [32]
$C_5H_3Me_2V(CO)_4$ [a]	−1515, −1520 [32]	R = Cy	−1521 [32]
$C_5H_2Me_3V(CO)_4$ [a]	−1503, −1507 [32]	R = C(HOH)Me	−1510 [32]
$C_5HMe_4V(CO)_4$	−1496 [32]	R = trityl	−1484 [36]
$C_5Me_5V(CO)_4$	−1492 [32]	R = C(NOH)Me	−1459 [32]
$C_5Br_5V(CO)_4$	−1029 [35]	R = C(O)Me	−1406 [32]
$C_5Cl_5V(CO)_4$	−1010 [35]	$C_5H_3Me(sBu)(CO)_4$, **39**[b]	−1517/−1526; −1527/−1535 [33]

[a] The two signals represent two positional isomers.
[b] The four signals belong to the four diastereomers shown in Scheme 9.

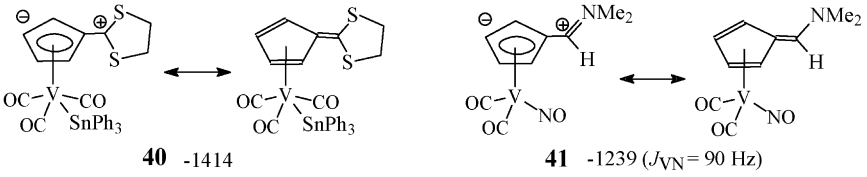

Scheme 11.

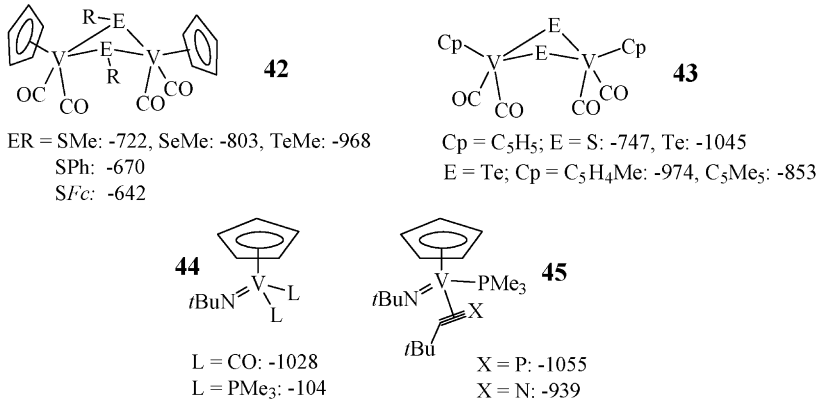

Scheme 12.

ER(1-) functions (E = group-16 element, R = methyl, phenyl or ferrocenyl), are strongly antiferromagnetically coupled and thus give distinct ^{51}V resonances. Contrasting dinuclear V^{IV} complexes with bridging chalcogenides (vide infra), shielding in type **42** (V^{II}) and **43** (V^{III}) compounds [39] (Scheme 12) increases as the softness of the bridging group increases [38]. The ring substituent effect, i.e. going from cyclopentadienyl to methyl- and pentamethyl-cyclopentadienyl, again parallels that observed in $\{CpV^{+I}\}$ carbonyl complexes. In the V^{III} complexes **44**, the dramatic decrease in shielding on replacing carbonyl for trimethylphosphine is noteworthy. In contrast, complex **45**, with PMe_3 and a heteroalkyne in place of the carbonyls, shielding again is in the expected range [25].

For the dinuclear $\{CpV^{IV}\}$ complexes **46** [40] and **47** [41] in Scheme 13, containing bridging chalcogenide(2-) and dichalcogenide(2-), consistently low shielding has been noted. In accord with predictions from the influence of the polarizability of the E_2^{2-} and E^{2-} (Section 2.1), shielding decreases in the series $S_2^{2-} > Se_2^{2-} > S^{2-} > Se^{2-} > Te^{2-}$ (**47a–d**), with **47c** (+2382) [39] exhibiting the lowest shielding so far observed for

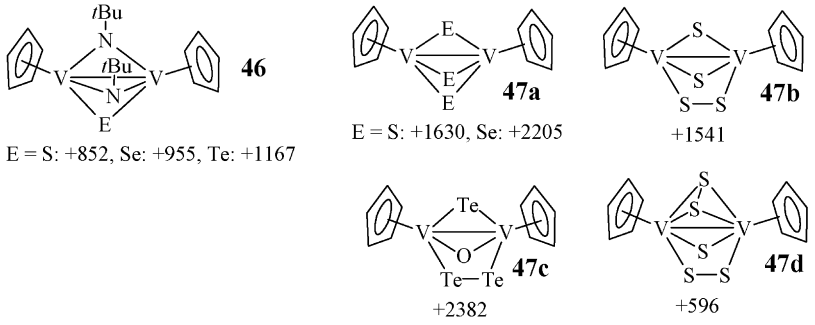

Scheme 13.

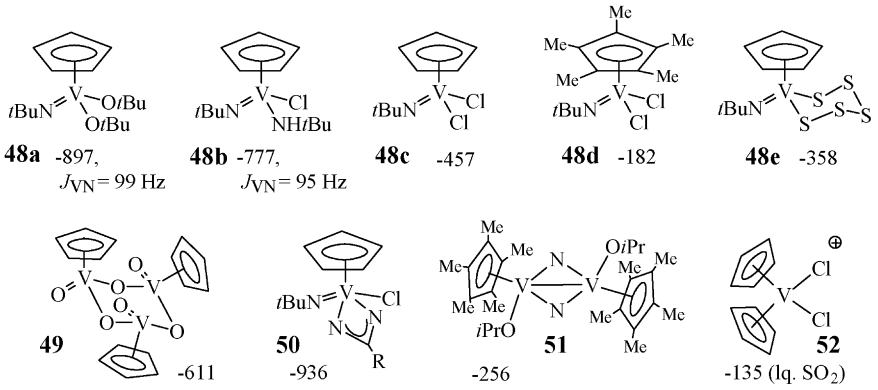

Scheme 14.

an organovanadium compound, outnumbered only by the inorganic tetraselenidovanadate $[VSe_4]^{3-}$ (+2570); cf. also Fig. 1.

In the $\{CpV^V\}$ complexes **48–52** in Scheme 14, vanadium is consistently more effectively shielded than in the μ-chalcogenido complexes **46** and **47**. As in inorganic high-valent vanadium compounds, shielding increases with increasing electronegativity (and decreasing polarizability) of the ligands composing the ligand sphere, i.e. OR (**48a** [43], **49** [45]) ≈ NHR (**48b** [43]) > Cl (**48c** [42]) > {S} (**48e** [40]). Expansion of the coordination sphere from 4 to 5, as in the benzamidinato complex **50**, gives rise to additional shielding [44]. The deshielding effect on going from C_5H_5(1-) to C_5Me_5(1-), **48c** versus **48d** [42], is again noted here. An interesting case is the dinuclear V^V complex **51**, which is best interpreted as a bis(μ-nitrido) complex with the binding electrons delocalized over the $V_2(\mu\text{-}N)_2$ core [46]. The tetrahedral cationic complex **52** (counter-ion is $[AsF_6]^-$) [47] once more reflects low shielding in the presence of chloro ligands.

4. Applications to catalysis

Compound **53** in Scheme 15, derived from **4a** (Schemes 1 and 15) by addition of trialkylaluminium, shows mild catalytic activity in olefin polymerization [9]. Density functional theory (DFT) calculations for the polymerization of ethene catalysed by the simplified version of **53**, the model catalyst **54b** (derived from **54a** by addition of AlH_3), yielded an activation barrier ΔE_a of 50 kJ/mol for the transition state (TS) of the ethylene insertion – **54b**$_{(TS)}$ in Scheme 15 – of 80 kJ/mol, about13 kJ/mol less than for **54a** [28,48]. Stronger Lewis acids

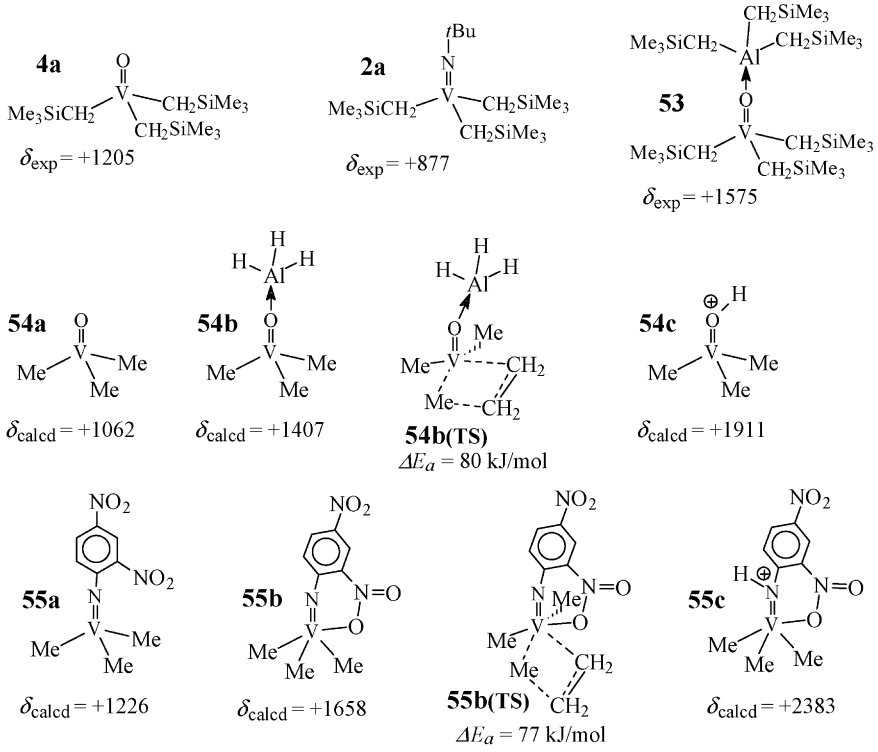

Scheme 15.

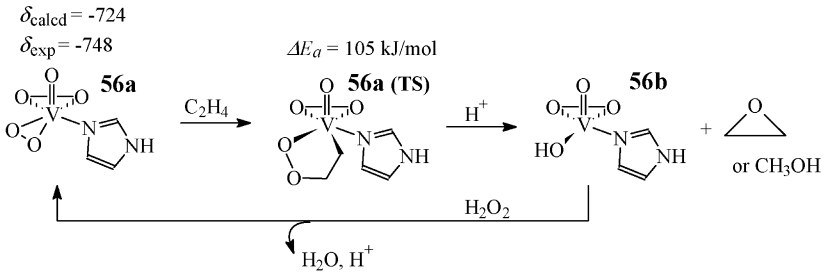

Scheme 16.

reduce ΔE_a, and a particularly low ΔE_a of 50 kJ/mol is obtained for protonation of the terminal oxo group (**54c**). Corresponding results have been obtained for model systems of compound **2a**, such as **55** in Scheme 15 [49]. Anchimeric assistance of the *o*-NO_2 group (**55b** vs. **55a**) reduces ΔE_a from 108 to 77 kJ/mol (**55b**$_{(TS)}$ in Scheme 14). A further reduction, to 49 kJ/mol, is achieved on protonation (**55c**). All these reductions of the insertion barrier go along with a decrease in shielding (Fig. 8), a finding which can be helpful in designing more efficient catalysts. Similar calculations have been carried out to reveal the possible pathway for epoxidations catalyzed by the peroxo complex **56a** (Scheme 16) [50]. The activation barrier for the cyclic intermediate **56a**$_{(TS)}$, 105 kJ/mol, is, however, substantially higher than for direct transfer of oxygen from **56a** to the substrate. Interestingly, the monoperoxo complex **56b** formed in the course of the hypothetic cycle depicted in Scheme 16 is closely related to the active centre intermediate present in the enzyme family vanadate-dependent haloperoxidases, which catalyze the oxygenation, by peroxide, of halides, thioethers and terpenes.

5. Epilogue

The data collated and discussed in Sections 3, 4 and 5 clearly indicate that ^{51}V NMR is a sensitive and versatile tool not only from an analytical point of view, but also in providing information on the electronic structure at the vanadium centre as imposed by ligand functions in the first coordination sphere, as well as by modulations of the electronic situation rooting in more distant coordination spheres. The latter influence, often a "substituent effect", can be particularly useful, when correlated with shielding data and supported by DFT calculations, in predicting catalytic activity and thus designing effective catalysts.

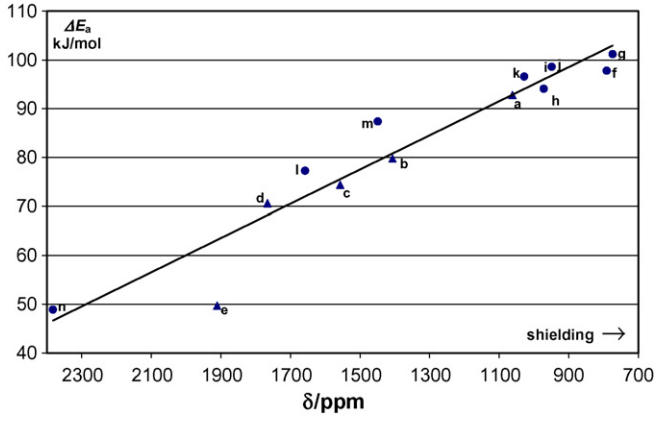

Fig. 8. Correlation between the ethylene insertion barriers ΔE_a and the calculated chemical shifts $\delta(^{51}V)$; data taken from Refs. [48,49]. (▲) Me_3VO (a) and Me_3VOX, X = AlH_3 (b), Li (c), SbF_5 (d) and H (e); (●) Me_3VNX, X = H (f), CMe_3 (g), $C(CF_3)_3$ (h), Ph (i), *p*-MeOPh (j), *p*-O_2NPh (k), 2,4-$(NO_2)_2$Ph (l), 4-NO_2-2-acylPh (m), $Me_3V\{N(H)2,4\text{-}(NO_2)_2Ph\}$ (n); (e) excluded from the linear regression.

The compilation provided in Fig. 1 undoubtedly shows that there is no simple correlation between ^{51}V shielding and the "electron density" (in the conventional, vivid sense) imparted by the surroundings, usually the ligand set. This conception, which might work pretty well in ^{1}H NMR (and, to some extent, still in ^{7}Li NMR), clearly is a misconception when it comes to heavier nuclei, including, of course, the nucleus ^{51}V. This misconception, which unfortunately is widespread, commonly leads to invalid conclusions when it relates to the interpretation of, e.g., substituent effects. At this point, it should also be pointed out again that shielding is solvent- and temperature-dependent (pressure also plays a role). Consequently, any comparison of shielding data within series of similar compounds presupposes comparable medium and temperature conditions.

Although this article has concerned itself mostly with organometallic vanadium complexes, the recent literature reveals an increasing interest in applications of ^{51}V NMR in classical coordination chemistry, as outlined in detail in a recent review [2]. In addition, the following recent references provide a brief introduction into this area and the reader is recommended to consult these and related literature for further examples:

- Oxovanadium(V) complexes of bis(phenolate) ligands with acetylacetone as co-ligand: synthesis, crystal structure, electrochemical and kinetic studies on the oxidation of ascorbic acid [51].
- Chiral dioxovanadium(V) complexes with single condensation products of 1,2-diaminocyclohexane and aromatic *o*-hydroxycarbonyl compounds: synthesis, characterization, catalytic properties and structure [52].
- Chelation of vanadium(V) by difluoromethylene bisphosphonate, a structural analogue of pyrophosphate [53].
- Vanadium(IV) and oxidovanadium(IV) and (V) complexes with soft thioether coordination; synthesis, spectroscopic and structural studies [54].
- Targeted synthesis of μ-oxo divanadium(V) compounds with asymmetry in coordination environments [55].

- V-51 NMR chemical shifts calculated from QM/MM models of vanadium chloroperoxidase [56].
- Synthesis and characterization of vanadium(IV) and (V) complexes with 2-hydroxy-acetophenone-semicarbazone (H_2hasc) as ligand. X-ray crystal structures of [VO_2(H_2hasc)] and [VO_2(Hhasc)] [57].
- On the fate of vanadate in human blood [58].
- Vanadium (IV and V) complexes of reduced Schiff bases derived from the reaction of aromatic *o*-hydroxyaldehydes and diamines containing carboxyl groups [59].

References

[1] O.W. Howarth, Prog. Nucl. Magn. Reson. Spectrosc. 22 (1990) 453.
[2] D. Rehder, T. Polenova, M. Bühl, Ann. Rep. NMR Spectrosc. 62 (2007) 49.
[3] (a) D. Rehder, Coordin. Chem. Rev. 110 (1991) 161;
(b) D. Rehder, in: P.S. Pregosin (Ed.), Transition Metal Nuclear Magnetic Resonance, Elsevier, Amsterdam, 1991, p. 1;
(c) D. Rehder, in: M. Gielen, R. Willem, B. Wrackmeyer (Eds.), Advanced Applications of NMR to Organometallic Chemistry, John Wiley & Sons, Chichester, 1996 (Chapter 10).
[4] (a) D. Rehder, M. Hoch, C.J. Jameson, Magn. Reson. Chem. 28 (1990) 128;
(b) D. Rehder, Magn. Reson. Rev. 9 (1984) 125.
[5] (a) F. Preuss, H. Becker, T. Wieland, Z. Naturforsch. 45b (1990) 191;
(b) F. Preuss, T. Wieland, B. Günther, Z. Anorg. Allgem. Chem. 609 (1992) 45.
[6] (a) C.C. Cummins, R.R. Schrock, W.M. Davis, Inorg. Chem. 33 (1994) 1448;
(b) C.P. Gerlach, J. Arnold, Inorg. Chem. 35 (1996) 5770.
[7] C.J. Jameson, D. Rehder, M. Hoch, J. Am. Chem. Soc. 109 (1987) 2589.
[8] S.J. Wolke, R. Buffon, U.P.R. Filho, J. Organomet. Chem. 625 (2001) 101.
[9] F.J. Feher, R.L. Blanski, Organometallics 12 (1993) 958.
[10] J. de With, A.D. Horton, A.G. Orpen, Organometallics 12 (1993) 1493.
[11] (a) F. Preuss, H. Becker, Z. Naturforsch. 41b (1986) 185;
(b) F. Preuss, M. Vogel, U. Fischbeck, J. Perner, G. Overhoff, E. Fuchslocher, F. Tabellion, B. Geiger, G. Wolmershäuser, Z. Naturforsch. 56b (2001) 1100.
[12] J. Yamada, K. Nomura, Organometallics 24 (2005) 3621.
[13] D.D. Devore, J.D. Lichtenhan, F. Takusagawa, E.A. Maatta, J. Am. Chem. Soc. 109 (1987) 7408.
[14] W.A. Herrmann, G. Weichselbaumer, H.J. Kneuper, J. Organomet. Chem. 319 (1987) C21.
[15] (a) F. Basuli, B.C. Bailey, D. Brown, J. Tomaszewski, J.C. Huffman, M.-H. Baik, D.J. Mindiola, J. Am. Chem. Soc. 126 (2004) 10506;
(b) J.-K.F. Buijink, J.H. Teuben, H. Kooijman, A.L. Spek, Organometallics 13 (1994) 2922.
[16] F. Preuss, G. Overhoff, H. Becker, J.H. Häusler, W. Frank, G. Reiß, Z. Anorg. Allgem. Chem. 619 (1993) 1827.
[17] J.-K.F. Buijink, A. Meetsma, J.H. Teuben, H. Kooijman, A.L. Spek, J. Organomet. Chem. 497 (1995) 161.
[18] J.-K.F. Buijink, A. Meetsma, J.H. Teuben, Organometallics 12 (1993) 2004.
[19] (a) F. Süßmilch, W. Glöckner, D. Rehder, J. Organomet. Chem. 388 (1990) 95;
(b) F. Süßmilch, F. Olbrich, H. Gailus, D. Rodewald, D. Rehder, J. Organomet. Chem. 472 (1994) 119;
(c) F. Süßmilch, F. Olbrich, D. Rehder, J. Organomet. Chem. 481 (1994) 125.
[20] (a) K. Ihmels, D. Rehder, Chem. Ber. 118 (1985) 895;
(b) K. Ihmels, D. Rehder, Organometallics 4 (1985) 1334.
[21] H. Gailus, H. Maelger, D. Rehder, J. Organomet. Chem. 465 (1994) 181.
[22] D. Rehder, Bull. Magn. Reson. 4 (1982) 33.
[23] J. Schiemann, E. Weiss, J. Organomet. Chem. 255 (1983) 179.
[24] (a) H.G. Alt, H.E. Engelhard, A. Razavi, D. Rausch, D. Rogers, Z. Naturforsch. 43b (1988) 438;
(b) B. Hessen, A. Meetsma, F. van Bolthuis, J.H. Teuben, Organometallics 9 (1990) 1925.
[25] M. Billen, G. Hornung, F. Preuss, Z. Naturforsch. 58b (2003) 975.
[26] B. Bachmann, F. Hahn, J. Heck, M. Wünsch, Organometallics 8 (1989) 2523.
[27] (a) D. Rehder, J. Magn. Reson. 38 (1980) 419;
(b) F. Näumann, D. Rehder, Z. Naturforsch. 39b (1984) 1647;
(c) F. Näumann, D. Rehder, V. Pank, Inorg. Chim. Acta 84 (1984) 117.
[28] M. Bühl, F.A. Hamprecht, J. Comput. Chem. 19 (1998) 113.
[29] R. Talay, D. Rehder, J. Organomet. Chem. 262 (1984) 25.
[30] (a) M. Hoch, D. Rehder, Inorg. Chim. Acta 111 (1986) L13;
(b) M. Hoch, Dissertation (Ph.D. Thesis), University of Hamburg, 1987.
[31] N.J. Coville, G.W. Harris, D. Rehder, J. Organomet. Chem. 293 (1985) 365.
[32] M. Hoch, D. Rehder, Chem. Ber. 121 (1988) 1541.
[33] D. Rehder, M. Hoch, M. Link, Organometallics 7 (1988) 233.
[34] D. Rehder, K. Paulsen, W. Basler, J. Magn. Reson. 53 (1983) 500.
[35] W. Priebsch, M. Hoch, D. Rehder, Chem. Ber. 121 (1988) 1971.
[36] M. Hoch, A. Duch, D. Rehder, Inorg. Chem. 25 (1986) 2907.
[37] D. Rehder, D. Wenke, J. Organomet. Chem. 348 (1988) 205.
[38] M. Herberhold, J. Peukert, M. Krüger, D. Daschner, W. Milius, Z. Anorg. Allgem. Chem. 636 (2000) 1289.
[39] M. Herberhold, M. Schrepfermann, J. Darkwa, J. Organomet. Chem. 430 (1992) 61.
[40] M. Billen, G. Hornung, G. Wolmershaeuser, F. Preuss, Z. Naturforsch. 58b (2003) 237.
[41] (a) M. Herberhold, M. Kühnlein, New J. Chem. 12 (1988) 357;
(b) M. Herberhold, M. Kühnlein, M. Schrepfermann, J. Organomet. Chem. 398 (1990) 259.
[42] F. Preuss, J. Perner, Z. Naturforsch. 55b (2000) 1.
[43] D. Gudat, U. Fischbeck, F. Tabellion, M. Billen, F. Preuss, Magn. Reson. Chem. 40 (2002) 139.
[44] F. Preuss, M. Scherer, C. Klingshirn, G. Hornung, M. Vogel, W. Frank, G. Reiß, Z. Naturforsch. 54b (1999) 1396.
[45] M. Herberhold, M. Schrepfermann, J. Organomet. Chem. 419 (1991) 85.
[46] T.S. Haddad, A. Aistars, J.W. Ziller, N.M. Doherty, Organometallics 12 (1993) 2420.
[47] P. Gowik, T.M. Klapoetke, K. Siems, U. Thewalt, J. Organomet. Chem. 431 (1992) 47.
[48] M. Bühl, Angew. Chem. Int. Ed. 37 (1998) 142.
[49] M. Bühl, Organometallics 18 (1999) 4894.
[50] M. Bühl, R. Schurhammer, P. Imhof, J. Am. Chem. Soc. 126 (2004) 3310.
[51] D. Maity, M. Mijanuddin, M.G.B. Drew, J. Marek, P.C. Mondal, B. Pahari, M. Ali, Polyhedron 26 (2007) 4494.
[52] E. Kwiatkowski, G. Romanowski, W. Nowicki, M. Kwiatkowski, S. Suwińska, Polyhedron 26 (2007) 2559.
[53] D.C. Crans, A.A. Holder, T.K. Saha, G.K.S. Prakash, M. Yousufuddin, R. Kultyshev, R. Ismail, M.F. Goodman, J. Borden, J. Florian, Inorg. Chem. 46 (2007) 6723.
[54] A.L. Hector, W. Levason, A.J. Middleton, G. Reid, M. Webster, Eur. J. Inorg. Chem. (2007) 3655.
[55] P.B. Chatterjee, N. Kundu, S. Bhattacharya, K.-Y. Choi, A. Endo, M. Chaudhury, Inorg. Chem. 46 (2007) 5483.
[56] M.P. Waller, M. Bühl, K.R. Geethalakshmi, D. Wang, W. Thiel, Chem. Eur. J. 13 (2007) 4723.
[57] P.I. da S. Maia, V.M. Deflon, G.F. de Sousa, S.S. Lemos, A.A. Batista, O.R. Nascimento, E. Niquet, Z. Anorg. Allgem. Chem. 633 (2007) 783.
[58] A. Gorzsás, I. Andersson, L. Pettersson, Eur. J. Inorg. Chem. (2006) 3559.
[59] J. Costa Pessoa, S. Marcão, I. Correia, G. Gonçalves, A. Dörnyei, T. Kiss, T. Jakusch, I. Tomaz, M.M.C.A. Castro, C.F.G.CX. Geraldes, A. Avecilla, Eur. J. Inorg. Chem. (2006) 3595.